AD-780 180

LOW CYCLE FATIGUE BEHAVIOR AND CRACK PROPAGATION IN SOME STEELS

Saurindranath Majumdar

Illinois University

Prepared for:

Advanced Research Projects Agency

April 1974

UILU-ENG 74 6009

T.&A.M. REPORT NO. 387

LOW CYCLE FATIGUE BEHAVIOR AND CRACK PROPAGATION IN SOME STEELS

by

Saurindranath Majumdar

Sponsored by

Advanced Research Projects Agency
ARPA Order No. 2169

DEPARTMENT OF THEORETICAL AND APPLIED MECHANICS
UNIVERSITY OF ILLINOIS
URBANA, ILLINOIS

T. & A. M. Report No. 387

LOW CYCLE FATIGUE BEHAVIOR AND CRACK PROPAGATION IN SOME STEELS

by

Saurindranath Majumdar

This research was performed in the Department of Theoretical and Applied Mechanics at the University of Illinois at Urbana-Champaign, Illinois 61801 with partial support of the Advanced Research Projects Agency of the Department of Defense under Grant Nos. DAHC 15-72-G-10 and DAHC 15-73-G-7; ARPA Order No. 2169 w/Amend. 1, Req. No. 1001/191; Methods and Applications of Fracture Control. The period of the Grants is from June 15, 1972 through June 14, 1974 and the amount is $100,000/year. Professor H. T. Corten 217/333-3175 is Principal Investigator and Professors G. M. Sinclair 217/333-3173, JoDean Morrow 217/333-4167 and H. R. Jhansale 217/333-1835 have participated as Project Scientists.

Department of Theoretical and Applied Mechanics
University of Illinois
Urbana, Illinois

April, 1974

ia

FOREWORD

Recent requirements for increased strength and service life of machines and structures have been met by the use of higher strength materials and new fabrication and joining methods. Simultaneously, failures due to fracture have increased relative to those resulting from excessive deformation. Frequently service conditions are such that low temperature brittle fracture, fatigue fracture, and high temperature creep rupture must be considered in a single system. National concern with increased safety, reliability, and cost has focused attention upon these problems.

Methods are now available to predict both fatigue crack initiation life and crack propagation life. Paradoxically the materials properties required for long fatigue crack initiation life are incompatible with the requirements of high fracture toughness. Thus, the conflicting design approaches and requirements placed on the material are confusing and often impossible to satisfy.

Numerous publications dealing with a variety of fracture problems have led to many new and useful developments. However, the synthesis of the concepts into methods for design, testing and inspection has lagged.

This program of study is intended to contribute to the integration, correlation, and organization of mechanics and materials concepts and research information into a form that will permit enlightened decisions to be made regarding fracture control. Reports are in preparation in three categories:

1. Research reports designed to explore, study and integrate isolated and/or conflicting concepts and methods dealing with life prediction,

2. Reports to introduce and summarize the state-of-the-art concepts and methods in particular areas, and

3. Example problems and solutions intended to illustrate the use of these concepts in decision making.

H. T. Corten

H. T. Corten
Principal Investigator

SUMMARY

In a previous report, a fatigue crack propagation model was analyzed by considering fatigue crack propagation as a sequence of fatigue crack initiation events. This permitted correlation to be made between the fatigue crack growth resistance and low cycle fatigue properties of metals.

Four steels were tested for low cycle fatigue behavior at the University of Illinois. Good correlation was obtained between the theoretically predicted crack propagation rate based on the measured low cycle fatigue properties of the four metals and experimentally observed crack propagation rates that were reported in the literature. Further, good estimates of crack propagation rates can be obtained on the basis of static tensile properties of the metals alone where cyclic properties are not available.

ACKNOWLEDGMENT

This study was performed in the H. F. Moore Fracture Research Laboratory of the Department of Theoretical and Applied Mechanics, University of Illinois at Urbana-Champaign. Support was provided by the Advanced Research Projects Agency of the Department of Defense under U. S. Department of the Army No. DAHC 15-72-G-10, ARPA Order No. 2169.

Professor H. T. Corten, Principal Investigator, and Professor J. Morrow, Faculty Associate, contributed to this research through helpful discussion and critical review of the manuscript. Mr. Dennis Dittmer, undergraduate research assistant, carried out all of the testing. Mrs. Darlene Mathine typed the manuscript. Special thanks are due to Dr. J. M. Barsom of U. S. Steel for sending us samples of the same steels used by him for crack propagation studies.

INTRODUCTION

Recently [1]* a fatigue crack propagation model was analyzed by considering fatigue crack propagation as a sequence of fatigue crack initiation events. This enabled the derivation of a fatigue crack propagation equation in terms of the low cycle properties of metals and a microstructure size. Good correlation between predicted crack propagation rates and experimentally observed values [2] was obtained for eight steels. However, due to lack of low cycle fatigue data, the predicted crack propagation rates were calculated on the basis of estimated low cycle fatigue properties.

Since the completion of the above report, Dr. J. M. Barsom of U. S. Steel Company has sent us samples for four of the eight steels used by him for crack propagation studies. Uniaxial specimens were prepared from these samples and tested in our laboratory for low cycle fatigue behavior. The present report contains the results of these tests and the recalculated values of the crack propagation rates based on the experimentally measured low cycle fatigue properties.

---

*Numbers in square brackets indicate references at the end of the report.

MATERIALS AND SPECIMENS

The following steels were tested:

(1) HY-80

(2) HY-130

(3) 10 Ni-Cr-Mo-Co

(4) 12 Ni-5 Cr-3 Co

Since the low life end (high strain range) of the spectrum was of primary interest, hourglass specimens, as shown in Fig. 1, were used to avoid buckling. All specimens were cut along the rolling direction and were machined to the form shown in Fig. 1 and polished mechanically.

APPARATUS AND PROCEDURE

All tests were performed in an axial closed loop servo controlled testing machine. Strain was measured diametrically at the minimum section of the specimen with a clip gage. The diametral strain signal was amplified and controlled between completely reversed limits. Axial loads were measured by a load cell in series with the specimen. An X-Y plotter was used to record the stress-strain hysteresis loops. Axial stress and stroke were continuously monitored. Hysteresis loops were plotted for the first few cycles and thereafter at regular intervals.

TEST PROGRAM

Tests were conducted at diametral strain amplitudes of ±0.1%, ±0.3%, ±1%, ±2%, ±3% and ±5%. In addition, a monotonic tension test was run for each material to determine the static tensile properties. The axial plastic strain amplitude was taken as twice the diametral plastic strain amplitude as obtained from half the width of the hysteresis loop, and the axial elastic strain amplitude was obtained by dividing the axial stress amplitude by the modulus of elasticity. To avoid necking, the tests at the largest two strain amplitudes were started with one cycle at ±1% followed by one cycle at ±2%. In most cases one specimen of each metal was tested at each strain amplitude level.

TEST RESULTS

Static tensile properties of the various metals are given in Table 1. Variation of stress amplitude with each cycle for all the tests are shown in Figs. 2-7. The 12 Ni steel softens at all strain amplitudes, but the other three steels soften at the lower strain ranges and harden at the highest two strain ranges. Virtually no cyclic plasticity was exhibited by the HY-130 steel at ±0.1% diametral strain amplitude. If steady state was not reached by the end of a test, the hysteresis loop at half the fatigue life was taken for plotting purposes. In all cases the stress amplitude dropped rapidly towards the end of the tests due to the presence of cracks. Cycles to initiate a crack was arbitrarily taken as the cycle at which the maximum load dropped by 5% from the steady state value.

Variation of stress amplitude with axial plastic strain amplitude are shown for all four metals in Fig. 8. Note that, when extended, these plots pass through the monotonic true fracture strength and ductility point. The cyclic strain hardening exponent of the metals varies from n' = 0.07 for 10 Ni to n' = 0.146 for HY-80. However, the power function applies over a wider range for the HY-80 and HY-130 steels as compared to the 10 Ni and 12 Ni steels.

Elastic, plastic and total strain amplitude versus reversals to failure for each metal are plotted on a log-log basis in Figs. 9-12. Best fit straight lines are drawn through the elastic strain amplitude versus reversals to failure and plastic strain amplitude versus reversals to failure points. Plastic strain amplitude versus reversals to failure for the 10 Ni and 12 Ni steels show a drop at low plastic strain amplitudes. For the purpose of the present report, these points are ignored in drawing the best fit straight line. The slope and the intercept at one reversal of the plastic strain amplitude versus reversals to failure line are defined as fatigue ductility exponent (c) and coefficient (ϵ_f') respectively. Fatigue strength coefficient (σ_f') and exponent (b) are similarly defined from the elastic strain amplitude versus reversals to failure plots. Various low cycle fatigue properties of the four metals are listed in Table 1 as well as in Figs. 9-12.

CRACK PROPAGATION RATES

Crack propagation rates for the four steels were calculated using Eq. (14) of [1] and the experimentally determined low cycle fatigue properties and the same "microstructure size" as in [1]. The results together with Barsom's test data [2] are shown in Figs. 13-16. The current calculated results are virtually the same as in [1]. A comparison of Table 1 with the Table on page 17 of [1] shows that the estimated values of the fatigue ductility exponent (c) and the product of the estimated value of fatigue strength and fatigue ductility coefficient (σ_f' ϵ_f') are fairly close to the measured values. Thus, although the other estimated low cycle fatigue properties vary somewhat from the present measured values, the computed crack propagation rates are insensitive to these variations. This is to be expected because Fig. 5 of [1] shows that the crack propagation rate is most sensitive to the variation in c, and the product $\sigma_f' \epsilon_f'$.

CONCLUDING REMARKS

In order to calculate crack propagation rates using Eq. (14) of [1], most of the low cycle fatigue properties need not be known very accurately. The fatigue ductility exponent (c) for most metals vary between -0.5 and -0.7 and may be estimated without great error. Estimates of the fatigue ductility and strength coefficients may be obtained from monotonic true fracture ductility and strength. Thus reasonable estimates for crack propagation rates may be computed from the usual monotonic stress-strain data.

REFERENCES

1. S. Majumdar and J. Morrow, "Correlation between Fatigue Crack Propagation and Low Cycle Fatigue Properties," T. & A. M. Report No. 364, University of Illinois at Urbana-Champaign, 1973. Also to be published as an ASTM STP for the Proceedings of the Seventh National Symposium of Fracture Mechanics, August, 1973.

2. J. M. Barsom, "Fatigue Crack Propagation in Steels of Various Yield Strengths," presented at the First National Congress of Pressure Vessels and Piping, San Francisco, California, May 10-17, 1971.

TABLE 1

MATERIAL PROPERTIES

	Monotonic Properties					Cyclic Properties				
Steel	Young's Modulus E ksi	Yield Strength* σ_y ksi	Ultimate Strength S_{ult} ksi	True Fracture Strength σ_f ksi	True Fracture Ductility ϵ_f	Cyclic Strain Hardening Exponent n'	Fatigue Strength Coefficient σ_f' ksi	Fatigue Strength Exponent b	Fatigue Ductility Coefficient ϵ_f'	Fatigue Ductility Exponent c
HY-80	28×10^3	105	123	203	1.23	0.145	196	-0.096	0.89	-0.62
HY-130	28×10^3	147	160	224	0.92	0.100	216	-0.060	0.90	-0.64
10 Ni	27×10^3	189	206	302	1.13	0.070	270	-0.053	1.25	-0.69
12 Ni	27×10^3	195	202	280	0.89	0.078	250	-0.050	0.96	-0.69

*0.2% offset

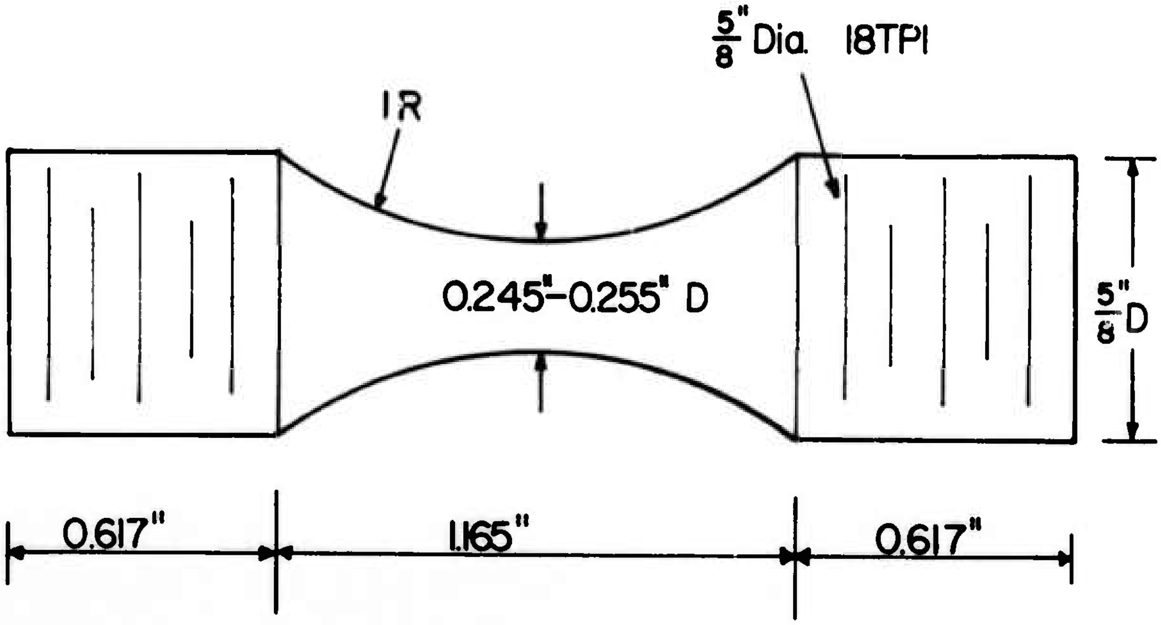

FIG. 1 GEOMETRY OF TEST SPECIMEN

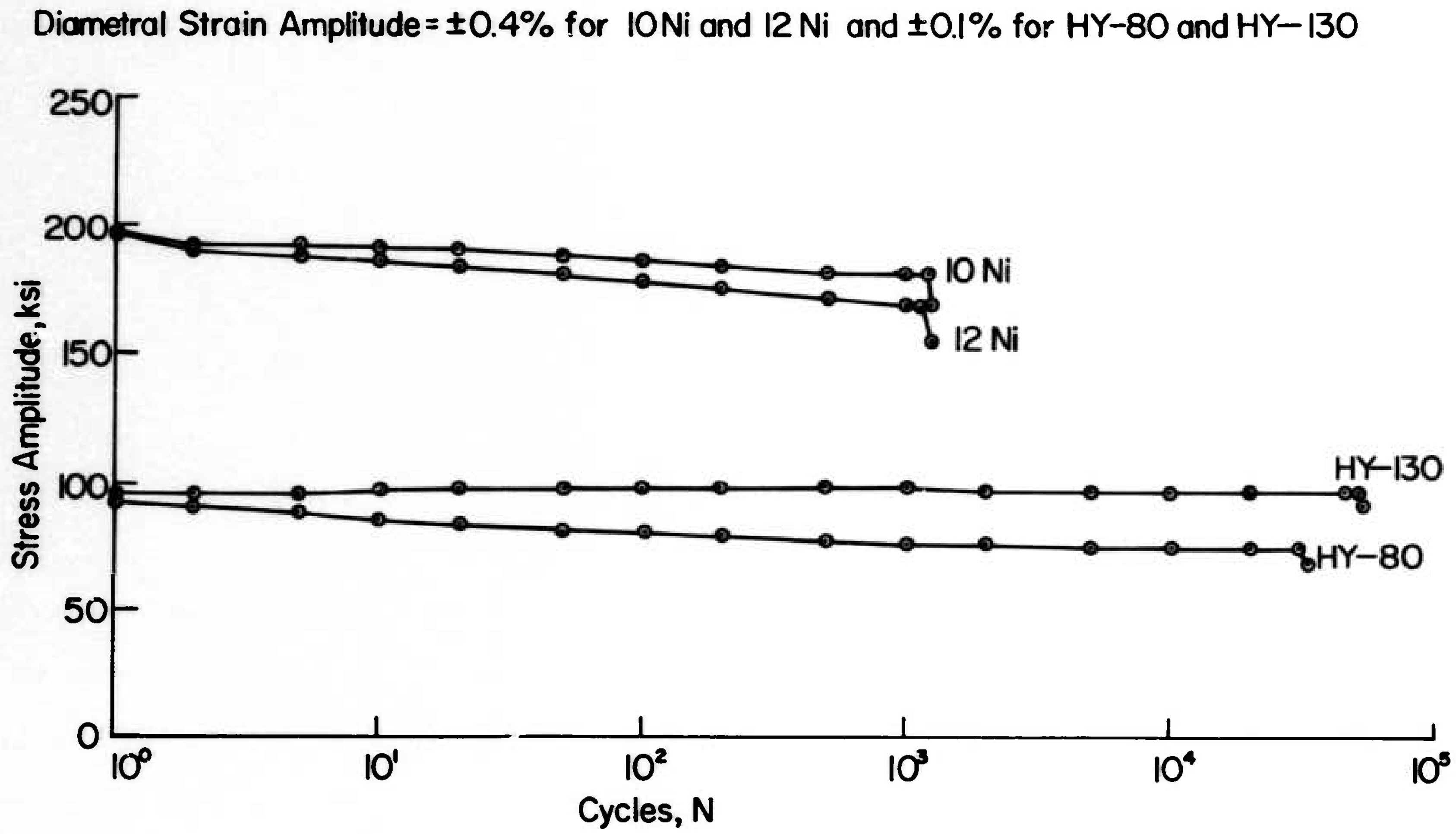

FIG. 2 VARIATION OF STRESS AMPLITUDE WITH CYCLES

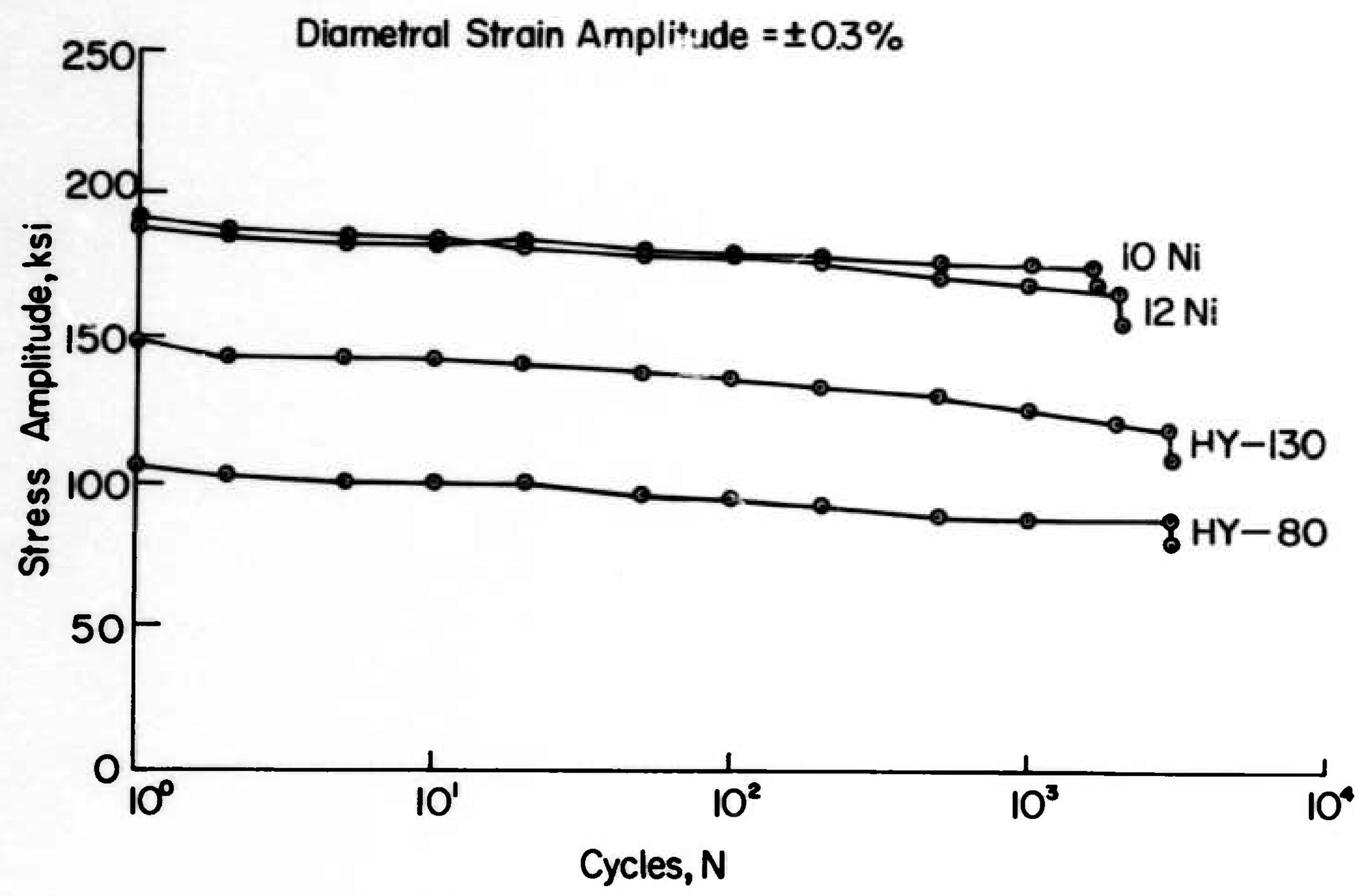

FIG. 3 VARIATION OF STRESS AMPLITUDE WITH CYCLES

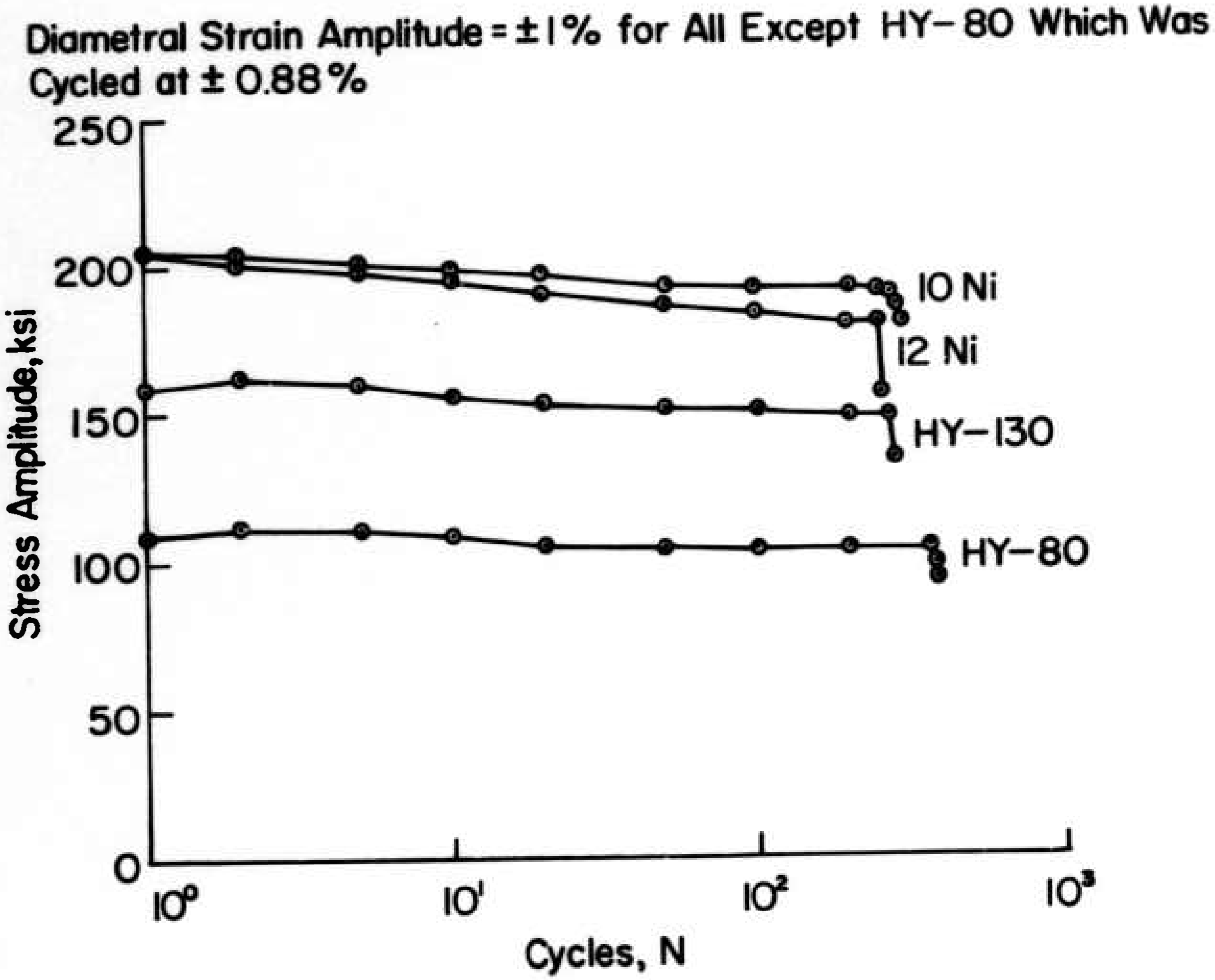

FIG. 4 VARIATION OF STRESS AMPLITUDE WITH CYCLES

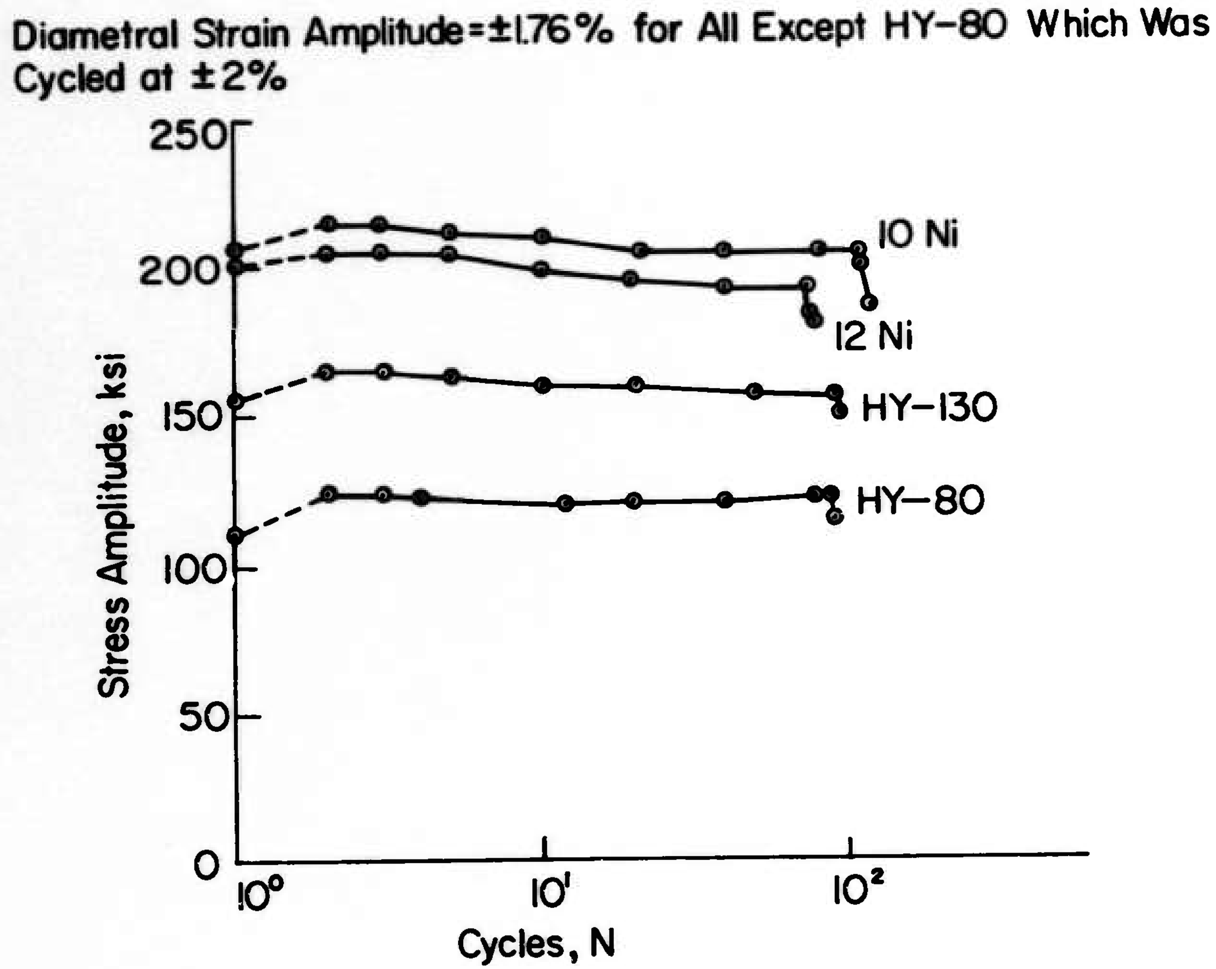

FIG. 5 VARIATION OF STRESS AMPLITUDE WITH CYCLES

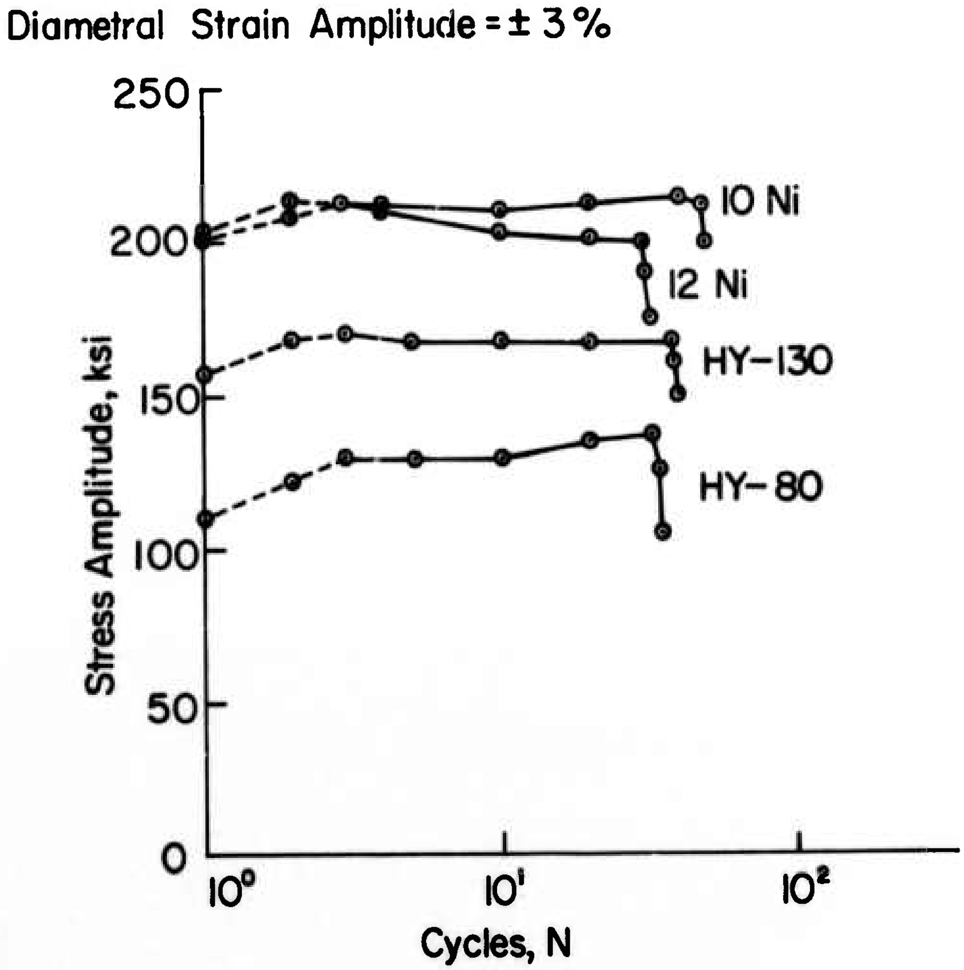

FIG. 6 VARIATION OF STRESS AMPLITUDE WITH CYCLES

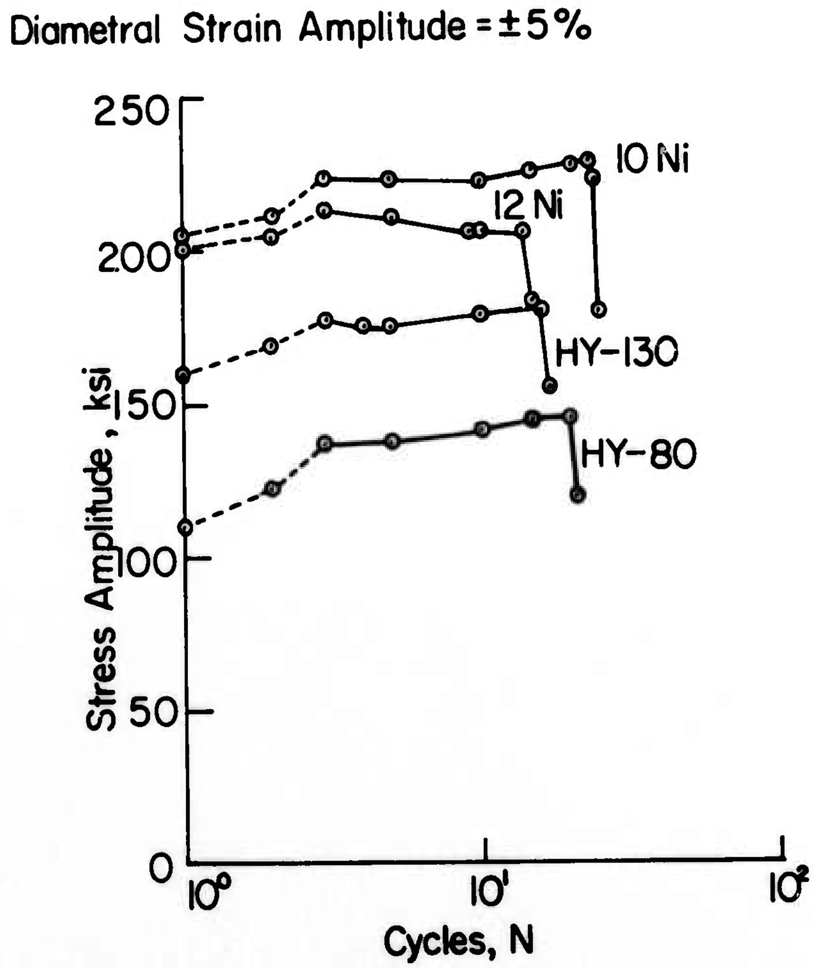

FIG. 7 VARIATION OF STRESS AMPLITUDE WITH CYCLES

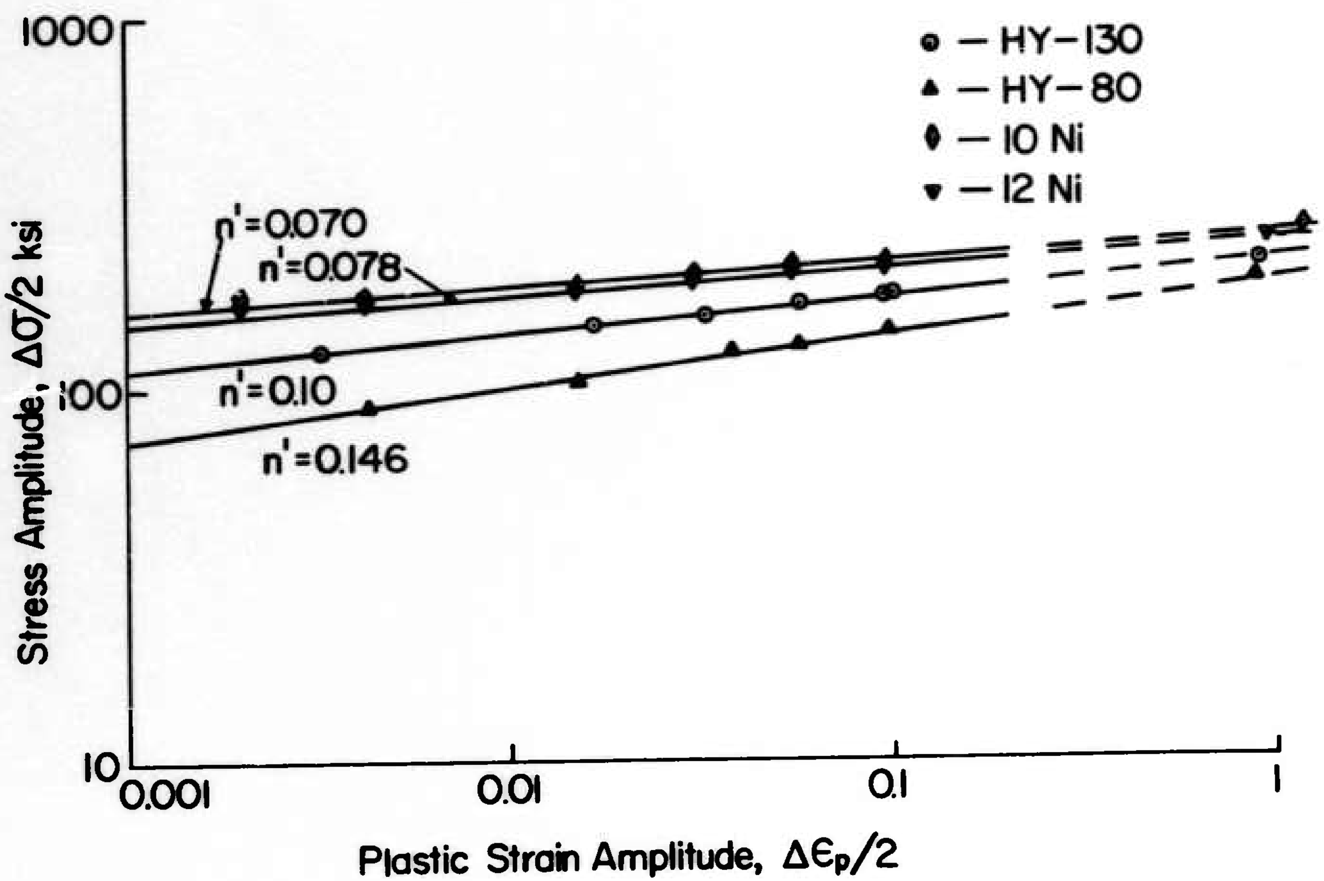

FIG. 8 CYCLIC STRESS-STRAIN CURVES

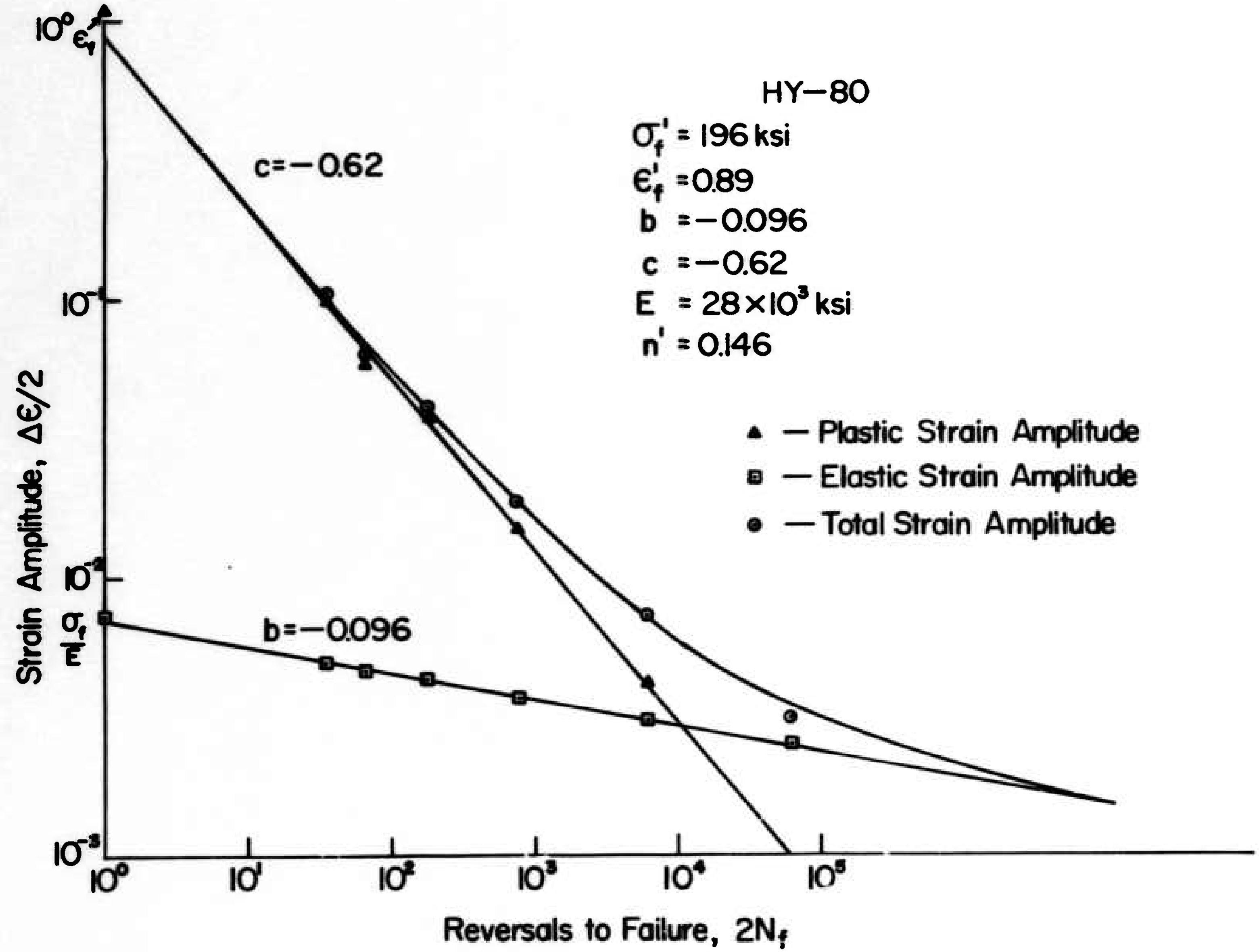

FIG. 9 STRAIN AMPLITUDE VERSUS REVERSALS TO FAILURE FOR HY-80

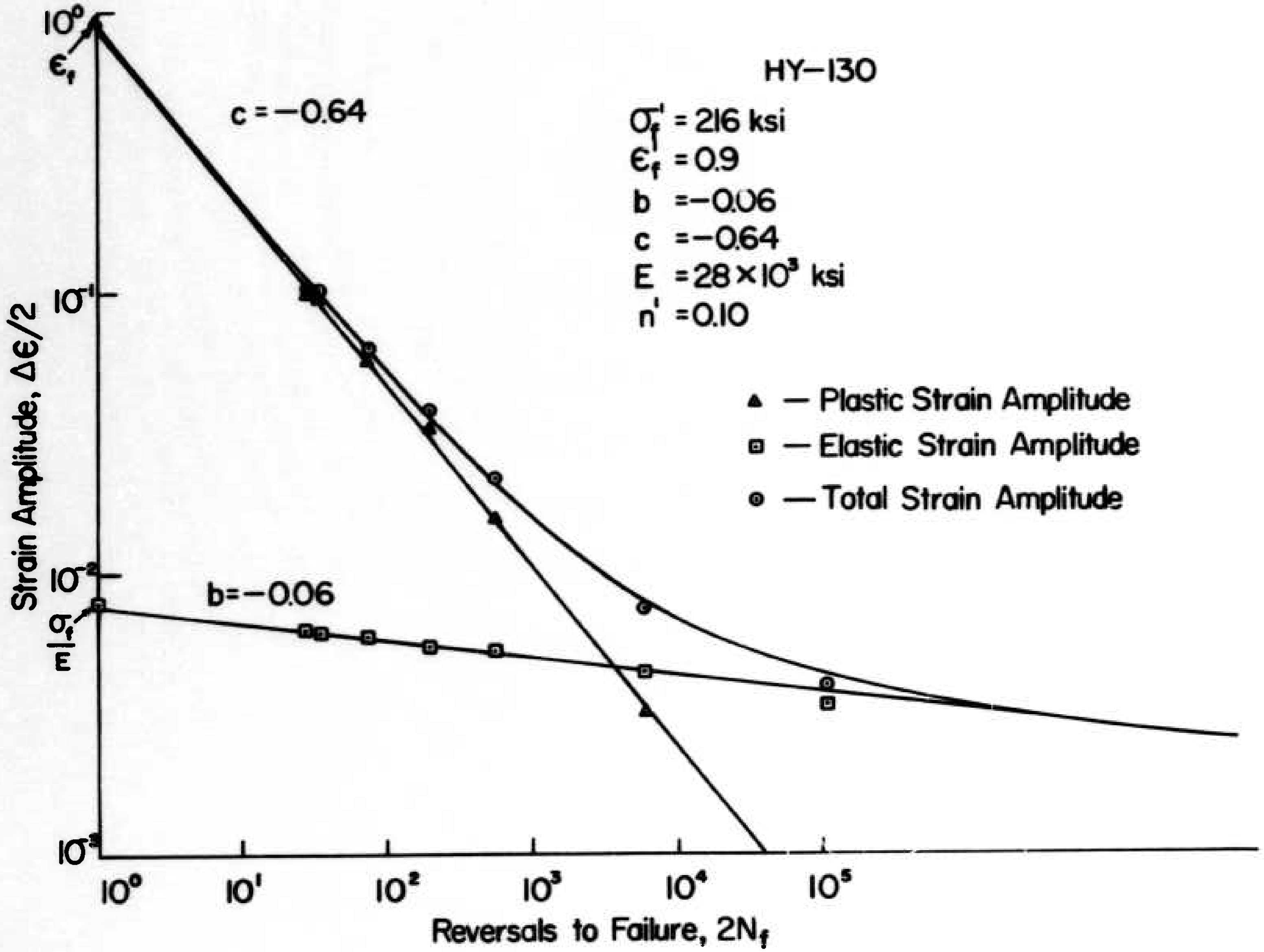

FIG. 10 STRAIN AMPLITUDE VERSUS REVERSALS TO FAILURE FOR HY-130

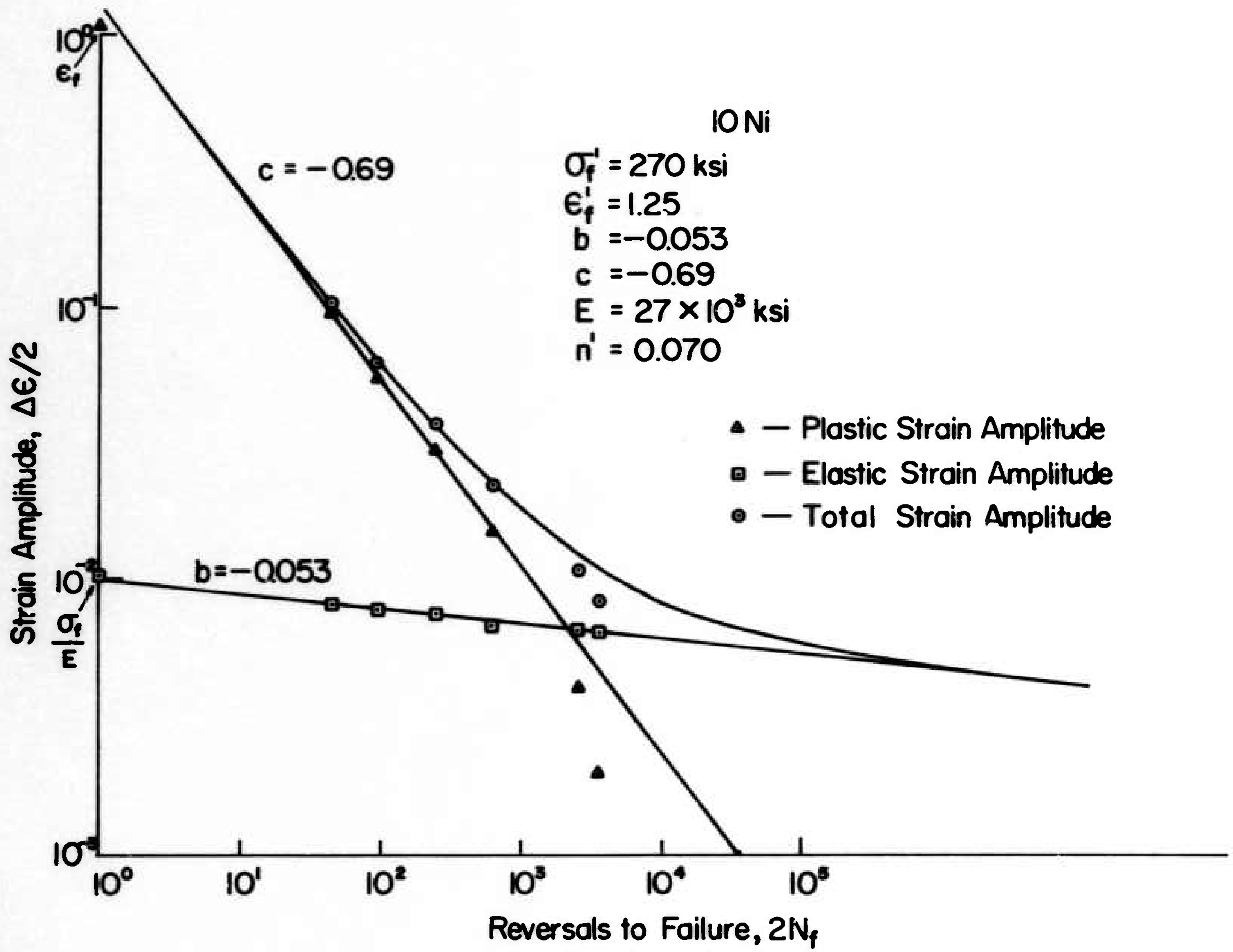

FIG. 11 STRAIN AMPLITUDE VERSUS REVERSALS TO FAILURE FOR 10 Ni

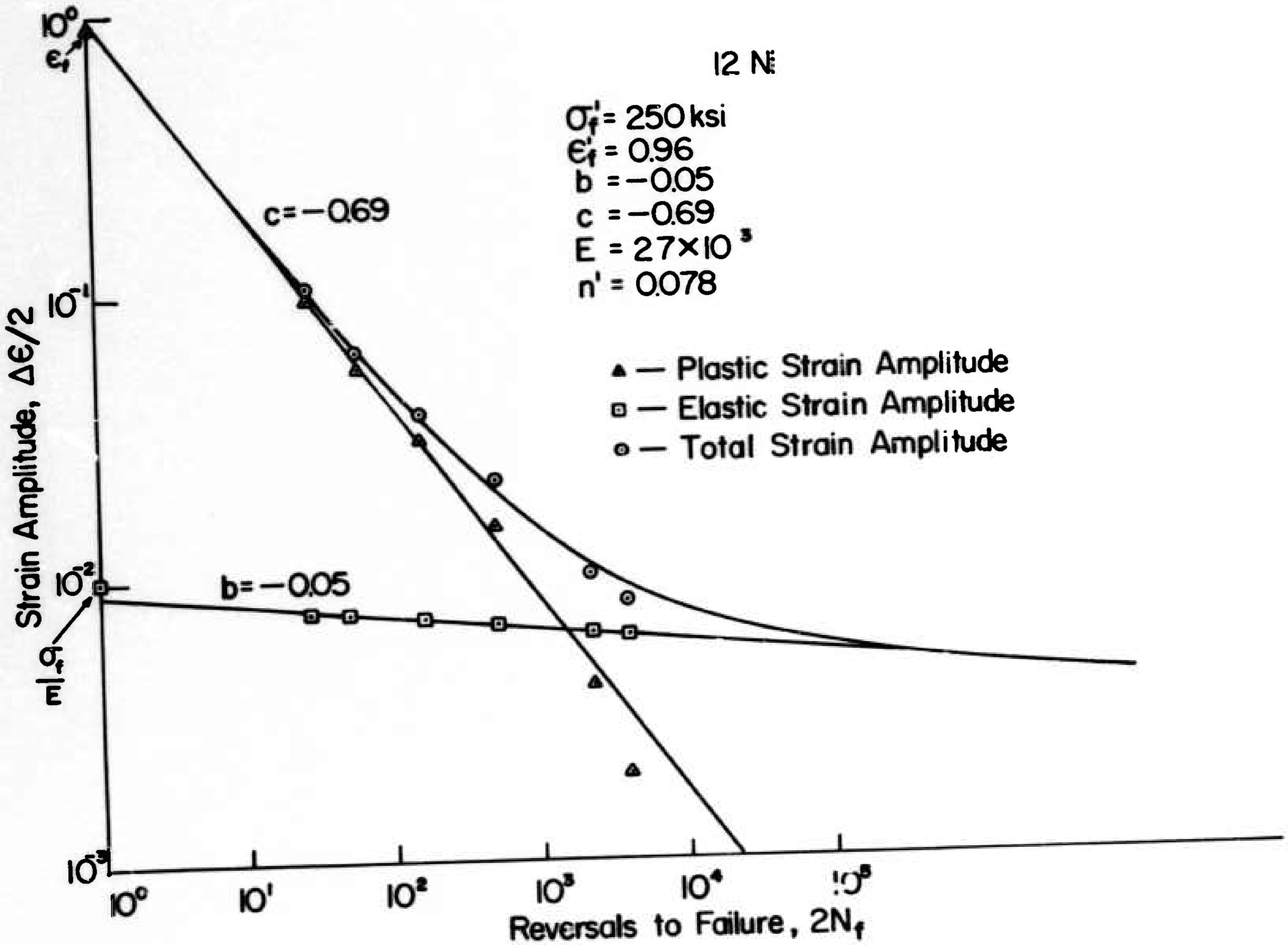

FIG. 12 STRAIN AMPLITUDE VERSUS REVERSALS TO FAILURE FOR 12 Ni

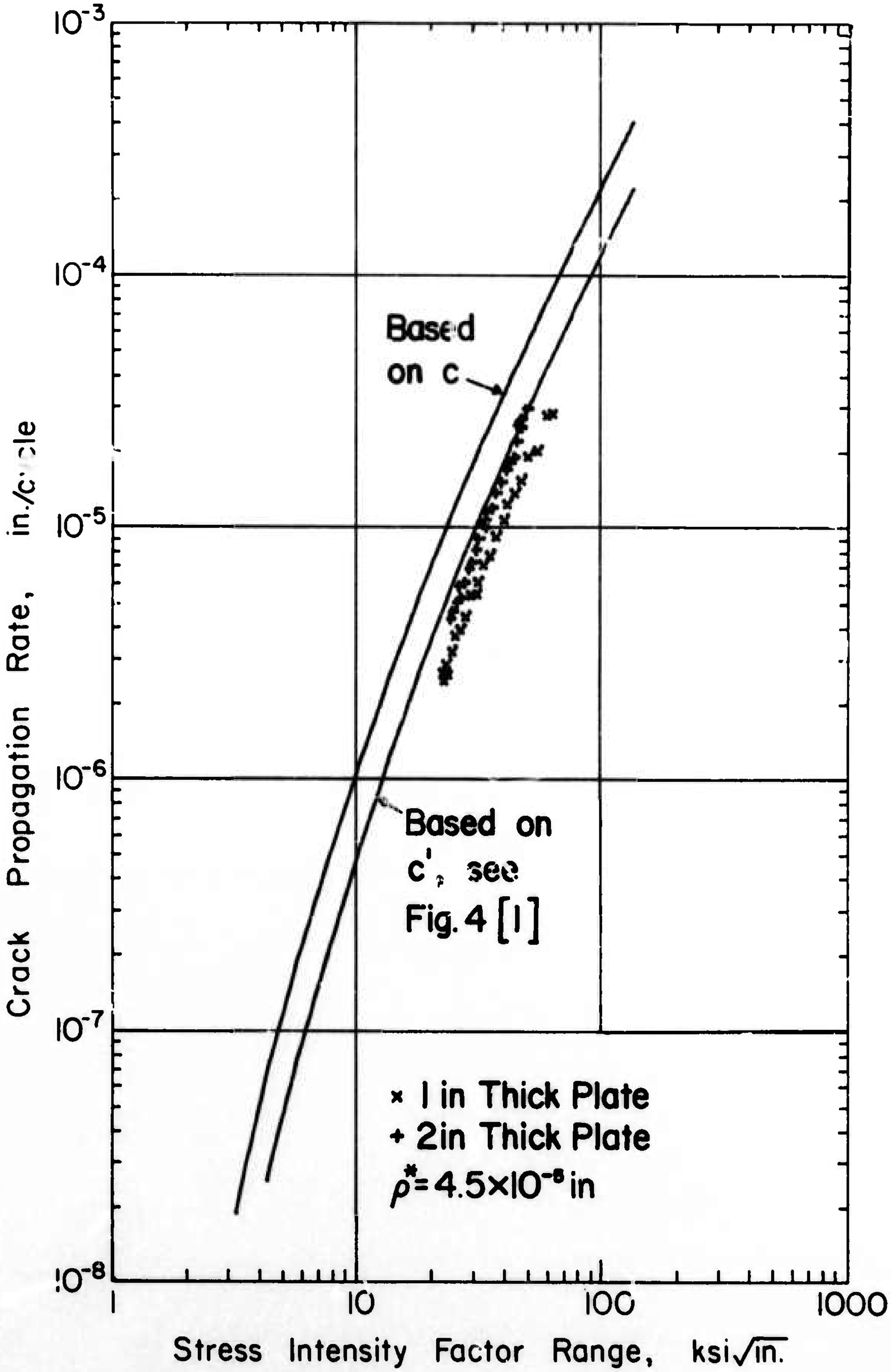

FIG. 13 COMPARISON OF EXPERIMENTAL DATA [2] WITH THEORETICAL PREDICTION FOR HY-80

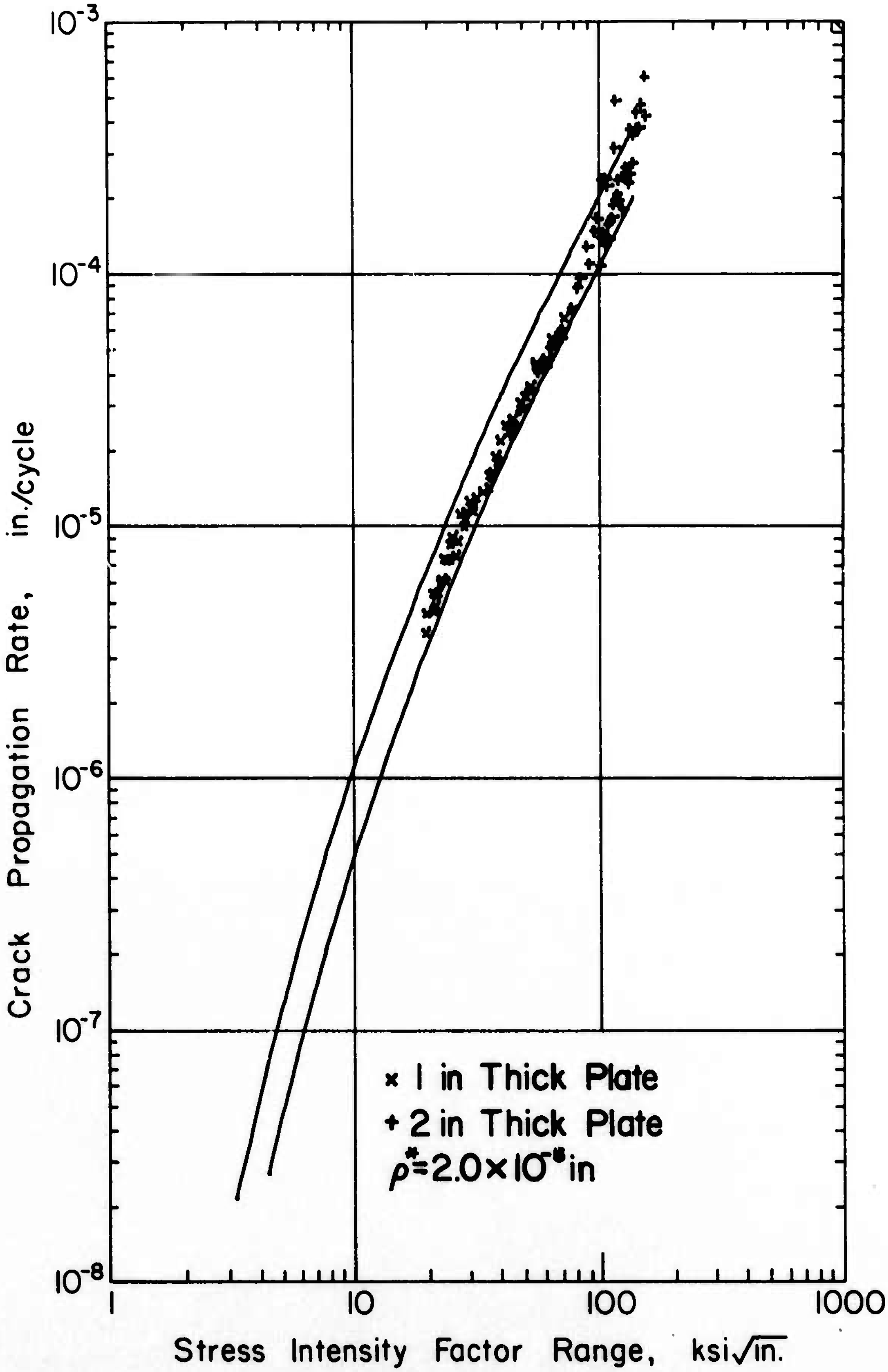

FIG. 14 COMPARISON OF EXPERIMENTAL DATA [2] WITH THEORETICAL PREDICTION FOR HY-130

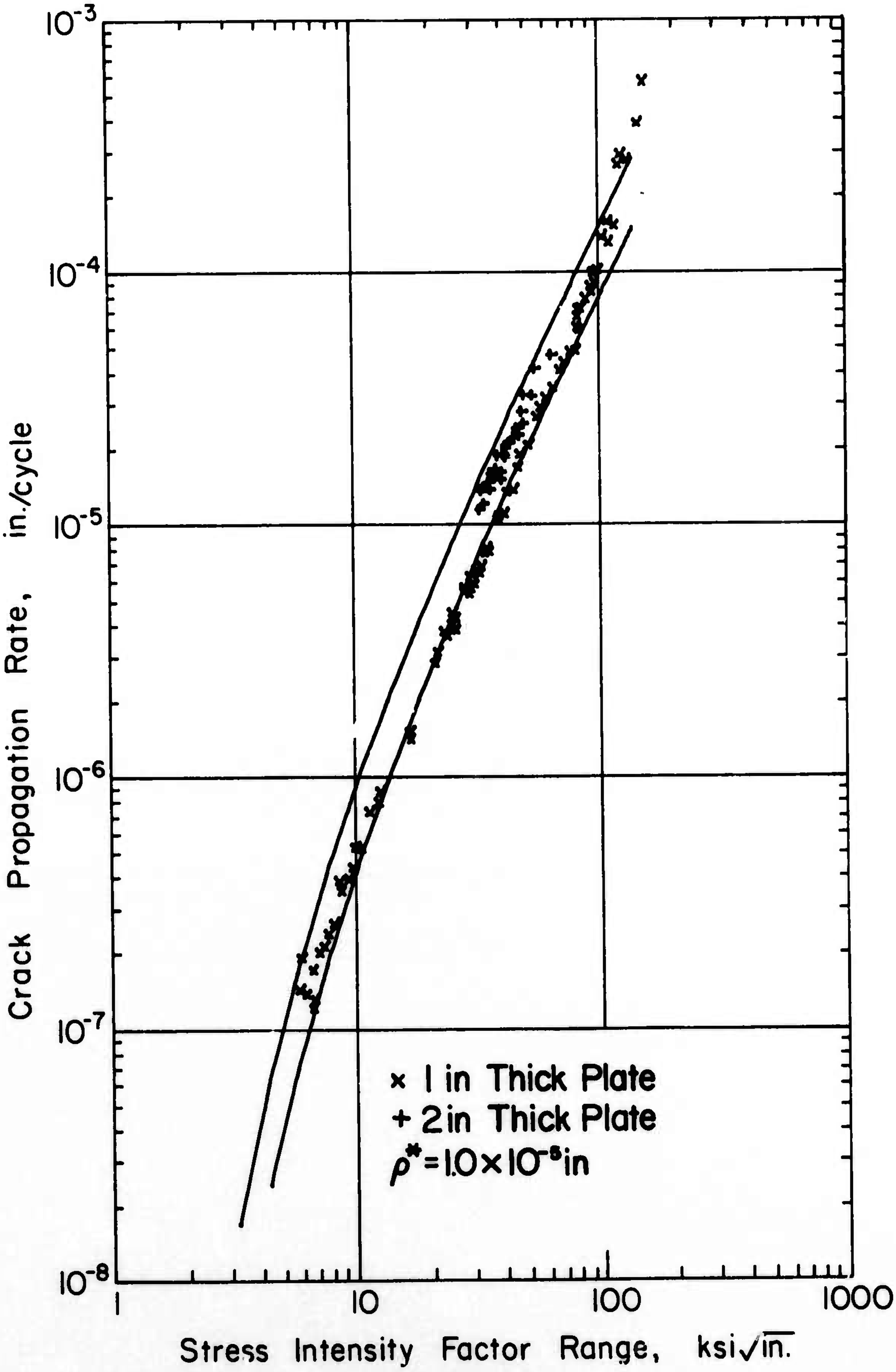

FIG. 15 COMPARISON OF EXPERIMENTAL DATA [2] WITH THEORETICAL PREDICTION FOR 10 Ni

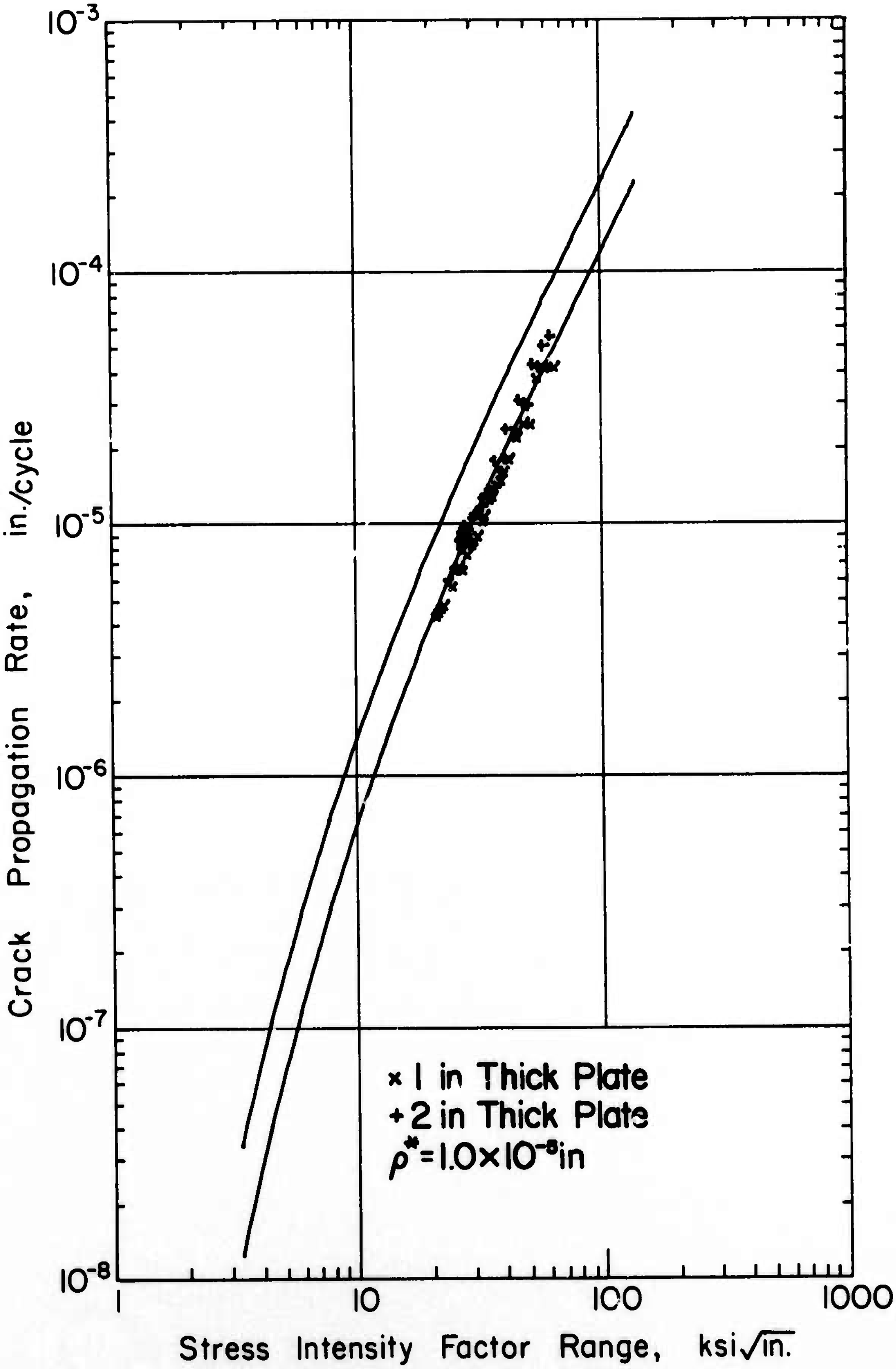

FIG. 16 COMPARISON OF EXPERIMENTAL DATA [2] WITH THEORETICAL PREDICTION FOR 12 Ni